Genetic Mosaicism in Calmodulinopathy

CIRCCVG2019002581 Revised June 2019

Lisa M. Wren, B.S.,[1] Juan Jiménez-Jáimez, M.D., Ph.D.,[2] Saleh Al-Ghamdi, M.D.,[3] Jumana Y. Al-Aama, M.D.,[4] Amnah Bdeir, Ph.D.,[4] Zuhair N. Al-Hassnan, M.D.,[5] Jyn L. Kuan, B.S.,[6] Roger Y. Foo, M.D.,[6] Franck Potet, Ph.D.,[1] Christopher N. Johnson, Ph.D.,[7] Miriam C. Aziz, B.S.,[8] Gemma L. Carvill, Ph.D.,[8] Juan-Pablo Kaski, M.D.,[9] Lia Crotti, M.D., Ph.D.,[10,11] Francesca Perin, M.D.,[12] Lorenzo Monserrat, M.D.,[13] Paul W. Burridge, Ph.D.,[1] Peter J. Schwartz, M.D.,[11] Walter J. Chazin, Ph.D.,[7] Zahurul A. Buihyan, M.B.B.S., Ph.D.,[14] and Alfred L. George, Jr., M.D.[1]

[1]*Department of Pharmacology, Northwestern University Feinberg School of Medicine, Chicago, Illinois; USA*
[2]*Cardiology Department, Virgen de las Nieves Hospital, Granada, Spain;*
[3]*Cardiac Sciences Department, Section of Pediatric Cardiology, King Abdulaziz Cardiac Center, Ministry of National Guard Health Affairs, Riyadh, Saudi Arabia*
[4]Princess Al Jawhara Albrahim Center of Excellence in Research of Hereditary Disorders, King Abdulaziz University, Jeddah, Saudi Arabia
[5]*The Cardiovascular Genetics Program, King Faisal Specialist Hospital & Research Center, Riyadh, Saudi Arabia*
[6]*Department of Cardiology, National University Heart Centre and Cardiovascular Research Institute, National University of Singapore, Singapore*
[7]*Department of Biochemistry and Center for Structural Biology, Vanderbilt University, Nashville, Tennessee; USA*
[8]*Department of Neurology, Northwestern University Feinberg School of Medicine, Chicago, Illinois; USA*
[9]*Institute of Cardiovascular Science, University College London, London, UK;*
[10]*Department of Medicine and Surgery, University of Milano-Bicocca, Milan, Italy*
[11]*IRCCS Istituto Auxologico Italiano, Center for Cardiac Arrhythmias of Genetic Origin and Laboratory of Cardiovascular Genetics, Milan, Italy;*
[12]*Pediatric Cardiology Division, Virgen de las Nieves Hospital, Granada, Spain;*
[13]*Cardiology Department, Health in Code SL, A Coruña, Spain;*
[14]*Laboratoire de Génétique Moléculaire, Service de Génétique Médicale, Centre Hospitalier Universitaire Vaudois (CHUV), Lausanne, Switzerland*

Short Title: *Mosaicism in calmodulinopathy*

Word Count: 6,116; 6 Figures; 1 Table; Supplement

Correspondence: Alfred L. George, Jr., M.D., Department of Pharmacology, Northwestern University Feinberg School of Medicine, Searle 8-510, 320 East Superior Street, Chicago, IL 60611, Tel: 312-503-4893, al.george@northwestern.edu

ABSTRACT

Background – Calmodulin (CaM) mutations are associated with congenital arrhythmia susceptibility (calmodulinopathy) and are most often *de novo*.

Objective – To broaden the genotype-phenotype spectrum of calmodulinopathies with two novel calmodulin mutations, and to investigate mosaicism in two affected families.

Methods – CaM mutations were identified in four independent cases by DNA sequencing. Biochemical and electrophysiological studies were performed to determine functional consequences of each mutation.

Results – Genetic studies identified two novel CaM variants (*CALM3*-E141K in two cases; *CALM1*-E141V) and one previously reported CaM pathogenic variant (*CALM3*-D130G) among four probands with shared clinical features of prolonged QTc interval (range 505 – 725 ms) and documented ventricular arrhythmia. A fatal outcome occurred for two of the cases. The parents of all probands were asymptomatic with normal QTc duration. However, two of the families had multiple affected offspring or multiple occurrences of intrauterine fetal demise (IUFD). The mother from the family with recurrent IUFD exhibited the *CALM3*-E141K mutant allele in 25% of next-generation sequencing reads indicating somatic mosaicism, whereas *CALM3*-D130G was present in 6% of captured molecules of the paternal DNA sample, also indicating mosaicism. Two novel mutations (E141K, E141V) impaired Ca^{2+} binding affinity to the C-domain of CaM. Human induced pluripotent stem cell (iPSC) derived cardiomyocytes overexpressing mutant or WT CaM showed that both mutants impaired Ca^{2+}-dependent inactivation (CDI) of L-type Ca^{2+}channels (LTCC) and prolonged action potential duration.

Conclusion – We report two families with somatic mosaicism associated with arrhythmogenic calmodulinopathy, and demonstrate dysregulation of the LTCC by two novel CaM mutations affecting the same residue. Parental mosaicism should be suspected in families with unexplained fetal arrhythmia or fetal demise combined with a documented CaM mutation.

Key words – arrhythmia, calmodulin, mosaicism, L-type Ca^{2+}channel

INTRODUCTION

Mutations in the Ca^{2+} sensing protein calmodulin (CaM) are associated with a spectrum of severe congenital arrhythmia susceptibility referred to as calmodulinopathy.[1-10] A common clinical presentation associated with CaM mutations is long QT syndrome (LQTS), which significantly increases the likelihood of arrhythmic events and sudden cardiac death (SCD) in the young. Other clinical presentations of calmodulinopathy have included catecholaminergic polymorphic ventricular tachycardia, idiopathic ventricular fibrillation, and sudden unexplained death. Most CaM mutations identified to date have been classified as *de novo* because the mutation is not detectable in the biological parents.

Calmodulin is a ubiquitously expressed protein that exhibits a high degree of evolutionary conservation.[11] There is also genomic redundancy within vertebrates as evidenced by the existence of three separate CaM genes (*CALM1*, *CALM2*, and *CALM3*) each encoding an identical 149 amino acid polypeptide.[12] CaM is composed of C-terminal and N-terminal domains, each with two Ca^{2+} binding EF-hand motifs, which are connected by a flexible linker helix.[13] Most identified human CaM mutations affect residues within the 3rd and 4th EF-hands in the C-domain, and most replace highly conserved residues essential for Ca^{2+} binding. Previous studies demonstrated that LQTS-associated CaM mutations cause impaired Ca^{2+} binding to the C-domain, dysregulation of LTCC inactivation, and prolongation of cardiac action potentials in a variety of cardiac cellular models.[7,14,15] Elucidating genotype-phenotype correlations and a complete mutation spectrum are expected to improve diagnostic accuracy, and enable stratification of patients for the most appropriate and mechanistically-guided therapy.

In this study, we report two novel mutations affecting the same amino acid residue in CaM encoded by either *CALM1* or *CALM3*. These cases provide further evidence of genotype-phenotype correlation in LQTS-associated calmodulinopathy with mutations that impair CaM Ca^{2+} binding affinity. Additionally, we report two families in which a pathogenic CaM mutation was inherited from a mosaic parent, which we believe are the first documented examples of mosaicism in calmodulinopathy. Recognizing mosaicism has important implications for family counseling in this disorder.

METHODS

All data, analytical methods, and study materials supporting this study are available from the corresponding author upon reasonable request for purposes of reproducing the results or replicating the procedures.

Study subjects and approvals

Genetic testing and review of medical records of Proband 1 was approved by the Local Ethics Committee of Virgen de las Nieves University Hospital. Approval for investigating Probands 2 and 4 were obtained from the Unit of Biomedical Ethics Research Committee, King Abdulaziz University. The parents of Proband 3 gave written informed consent for molecular studies and research using a consent document approved by the IRCCS Istituto Auxologico Italiano.

A full description of the methods is provided in the online Supplemental Material.

RESULTS

Clinical presentations

Proband 1 (Family A) was a Spanish female diagnosed with fetal sinus bradycardia at 16 weeks' gestation. ECG at birth demonstrated profound bradycardia (61 bpm) and 2:1 AV block with markedly prolonged QTc intervals (725 ms; **Fig. 1A**). There were transient episodes of T-wave alternans (**Fig. 1B**). Propranolol was administered at 3 mg/kg. The family history was negative for LQTS and diseases of cardiac conduction, and both parents had normal resting ECG traces (father, 410 ms; mother 422 ms). On the 23rd day of life, the proband had a cardiac arrest. The parents initiated CPR and promptly called emergency services. The initial ECG at the time of resuscitation showed VF, and an external shock (9 joules) restored sinus rhythm (**Fig. 1C**). Treatment with mexiletine (13 mg/kg) and flecainide (5 mg/kg) was initiated, but then stopped when no changes in the QTc interval were observed.

An epicardial cardioverter defibrillator (ICD) was implanted. She experienced two appropriate ICD discharges at age 3 years while on propranolol. Echocardiogram demonstrated left atrial dilatation and findings suggestive of left ventricular noncompaction. At age 4 years, the proband developed symptomatic hypoglycemia and propranolol dose was reduced to 2 mg/kg/day. However, at age 5 years, she had hypoglycemic coma and died. The parents later attempted to have more children. The mother reported three spontaneous miscarriages, and they voluntarily interrupted two other pregnancies because of fetal bradycardia in one case and spina bifida in the other (**Fig. 2A**). They later conceived two healthy sons with normal ECG recordings. DNA from the interrupted pregnancies and the healthy sons was not available for genetic testing.

Proband 2 (Family B) is a male offspring of unrelated parents from Saudi Arabia who had bradycardia (45-60 bpm) detected 12 hours after an uncomplicated birth. ECG demonstrated

bradycardia, and prolonged QTc intervals (660 ms; **Fig. 1D**). He was initially treated with propranolol without change in the QTc duration. Approximately 10 weeks later, a pacemaker was implanted because of syncope and recurrent 2:1 AV block, and he was paced initially at 100 bpm. However, there was failure to capture paced beats attributed to prolonged refractory period. Pacing rate was lowered to 60 bpm, propranolol dose was adjusted and mexiletine was added with resumption of sinus rhythm at an intrinsic rate of 90 bpm. Echocardiogram showed normal systolic function. At 21 months of age, he was clinically well without episodes of syncope. Both parents and a non-identical twin sister had no symptoms and normal ECGs including normal QTc duration (**Fig. 2B**).

Proband 3 (Family C) is a 7 year-old Maltese boy who suffered a first syncopal episode at 28 days of life. An ECG performed at that time was remarkable for a QTc > 500 ms, but the patient was not treated. At 18 months he suffered a second syncopal episode while breast feeding. A new ECG at that time demonstrated a QTc of 630 ms and deeply inverted T waves in the precordial leads. LQTS was diagnosed and propranolol therapy was started. Echocardiogram showed a structurally normal heart with good biventricular function. One month later, a single chamber ICD was implanted (**Fig. 1E**). During the ensuing 6 months, he had two episodes of loss-of-consciousness with detection of VT/VF correctly treated with ICD shocks. For three months, mexiletine was added to propranolol therapy, but it was not tolerated and was stopped. At age 3 years, propranolol dose was increased to 3 mg/kg/d. Left cardiac sympathetic denervation was considered but deferred because the child was not having further events. The family history was negative for cardiac events and the QTc of both parents was normal (**Fig. 2C**).

Proband 4 (Family D), the 6th child of consanguineous parents, presented with several episodes of self-terminating torsades de pointes during the first week of life. After hospitalization, he had

multiple episodes of ventricular arrhythmia for which he received DC shocks and required mechanical ventilation. He was treated with high dose propranolol, magnesium, lidocaine and later mexiletine. ECG recorded 4 days after birth demonstrated a prolonged QTc interval (505 ms; **Fig. 1F**) with 2:1 AV block. A pacemaker was implanted during his second week of life and he became clinically stable. He did well despite a persistent QTc > 600 ms on a regimen of propranolol, mexiletine and pacing at 60 bpm until age 4 years when he died suddenly.

Family history was notable for sudden death in four siblings (**Fig. 2D**). The first sibling had a seizure disorder treated with anticonvulsants starting at age 3 years, then died suddenly at age 6 years. The second child died suddenly at age 45 days. The third child was asymptomatic at age 13 years. The fourth child had fetal bradycardia and was delivered prematurely at 7 months gestation. After birth, the child exhibited LQTS with 2:1 AV block and died suddenly 10 days after birth following implantation of an ICD. The fifth child also had LQTS with 2:1 AV block detected after birth and died suddenly at age 45 days. There was no family history of deafness. The parents, who are closely related, were healthy with normal ECGs.

A summary of clinical and genetic features of the four cases is provided in Table 1.

Discovery of novel CaM mutations and parental mosaicism

Genetic testing of Proband 1 for mutations in *KCNQ1, KCNH2, SCN5A, KCNE1, KCNE2, KCNJ8, CAV3*, and *SCN4B* was negative. Later testing of the three calmodulin genes demonstrated a novel heterozygous variant in *CALM3* (c.421G>A; p.Glu141Lys; E141K; **Fig. 2E**). The variant affects the first nucleotide of *CALM3* codon 141 (GAG to AAG), which is the last base pair of exon 5. The variant was absent in the father and was not observed in the Genome Aggregation Database (gnomad.broadinstitute.org). However, the mother carried the *CALM3* variant in peripheral blood cells, but only in ~25% of next-generation sequencing reads,

which is consistent with somatic mosaicism and presumed germline mosaicism due to transmission of the variant. The mother's basal and exercise ECG traces were normal, and she never experienced an arrhythmic event.

Proband 2 was also discovered to be heterozygous for *CALM3*-E141K. The variant was absent in both parents and his unaffected, non-identical twin sister consistent with a *de novo* mutation. Genetic testing of Proband 3 revealed a novel heterozygous nonsynonymous variant in *CALM1* (c.422A>T; p.Glu141Val; E141V**; Fig. 2E**), which was absent in both parents consistent with a *de novo* mutation. This variant affects the second nucleotide of *CALM1* codon 141 (GAA to GTA, which is the first base pair of exon 6. The variant was not observed in the Genome Aggregation Database.

Initial screening of *KCNQ1* and *KCNH2* genes in Proband 4 revealed no mutations. Subsequent exome sequencing demonstrated a previously reported heterozygous *CALM3* mutation (c.389A>G; p.Asp130Gly, D130G).[16] This mutation was confirmed by Sanger sequencing and also demonstrated in the deceased fourth sibling, but neither parent was found to have the variant by exome sequencing (read depth at this nucleotide position was 43-46x). Other variants in other known arrhythmia susceptibility genes (*SCN5A*, *ANK2*, *AKAP9*) or paralogs (*ANK3*) discovered by exome sequencing did not segregate with the phenotype (**Supplemental Table S1**). Because of recurrence of this mutation in the family, we investigated the parents and healthy sibling for evidence of mosaicism using single molecule molecular inversion probes,[17] which offer the advantage over other next generation sequencing approaches by use of a unique molecular identifier (UMI) to detect mosaicism with greater sensitivity. We detected the c.389A>G variant in Proband 4 at constitutive levels (minor allele frequency 0.5), and this variant was absent in the mother and unaffected sister (II.3). However, we detected the c.389A>G variant in 3/84, 5/89, and 5/63 discrete triplicate captures (molecules) in paternal

DNA, correlating with a minor allele frequency of 0.056 (range 0.036-0.079). This result is consistent with somatic mosaicism in the father. Due to transmission of this variant to the affected children, germline mosaicism is assumed.

Novel CaM mutants impair Ca^{2+} binding affinity

Amino acid sequence alignments illustrate that the novel mutations E141K and E141V affect a strictly conserved glutamate residue within the fourth Ca^{2+} binding EF-hand motif of the CaM C-domain (**Fig. 3A**). Because the glutamate side chain directly chelates the Ca^{2+} ion in this site, we investigated whether E141K and E141V impair Ca^{2+} affinity using a previously described fluorescence assay. Inspection of raw Ca^{2+} binding data revealed diminished amplitude of fluorescence change for E141K and E141V relative to WT CaM, which suggests the mutated C-domain binds Ca^{2+} ions weakly (**Fig. 3B**). The Ca^{2+} binding affinities (Kd) for WT, E141K, and E141V CaM C-domain determined from normalized binding data were 2.3 ± 0.2 μM, 75 ± 7 μM, and 54 ± 4 μM, respectively (**Fig. 3C**). There were no significant differences in the Ca^{2+} affinities of the CaM N-domain (**Supplemental Fig. S1A**). A previous report demonstrated that CaM-E141G also impairs C-domain Ca^{2+} binding affinity to a lesser extent (K_d = 27 ± 0.5 μM).

We investigated the conformational changes associated with Ca^{2+} binding in more detail for the E141V and E141K mutations. Two-dimensional ^{15}N-^{1}H NMR spectra show that in the absence of Ca^{2+}, E141V and E141K protein backbones adopt nearly identical folded structures that are similar to WT apo-CaM (**Supplemental Fig. S1B**). In the presence of Ca^{2+}, many of the signals arising from residues in the CaM C-domain are reduced in intensity or significantly shifted, indicating that Ca^{2+} binding is impaired in mutated proteins (**Supplemental Fig. S1C,D**). Our results are consistent with previous studies of a mutation of the corresponding strictly conserved glutamate residue in position 12 of the EF-hand Ca^{2+} binding loop in calbindin D_{9k}, which showed that the mutated EF-hand is unable to attain the conformation of the WT EF-hand when

a Ca^{2+} ion is fully engaged.[18]

Novel CaM mutants affect Ca^{2+}-dependent inactivation of L-type Ca^{2+} channels

A primary mechanism proposed for calmodulinopathy-associated LQTS is dysregulation of L-type Ca^{2+} channels (LTCC) secondary to impaired Ca^{2+}-dependent inactivation (CDI).[7,14] To determine the effect of E141K and E141V on CDI, we recorded endogenous L-type Ca^{2+} currents in human iPSC-CM transiently transfected with WT or mutant CaM. **Figure 4A** illustrates representative Ca^{2+} current traces evoked by 100-ms depolarizing voltage steps from -80 mV to 60 mV recorded from human iPSC-CM expressing WT or mutant CaM. There are obvious differences in the time course and extent of Ca^{2+} current decay over time indicating that channel inactivation is slower and less complete for both E141K and E141V expressing cells. Current-voltage plots further demonstrate significant differences in peak (**Fig. 4B**) and late (**Fig. 4C**) Ca^{2+} currents in cells expressing mutant compared to WT CaM.

Figure 5A illustrates averaged normalized Ca^{2+} and Ba^{2+} current traces recorded at +10 mV from cardiomyocytes transfected with WT or mutant CaM. The WT CaM-expressing cells exhibit discordant time courses of current decay between Ca^{2+} and Ba^{2+} current traces indicative of CDI, which is blunted substantially in cells transfected with E141K or E141V. Cells expressing either E141K or E141V exhibit significantly larger inactivation time constants than cells expressing WT CaM when Ca^{2+}, but not Ba^{2+}, is the permeating ion (**Supplemental Fig. S2**). Impaired CDI is also evident in comparisons of Ca^{2+} current recorded at 100 ms (I_{end}) and normalized to the peak current (I_{peak}). Larger I_{end}/I_{peak} ratios indicate impaired CDI. The I_{end}/I_{peak} ratios are significantly larger for E141K and E141V compared to WT expressing cells across all tested voltages (**Fig. 5B**). These results indicate that E141K and E141V cause impaired CDI.

Effect of novel CaM mutants on the cardiac action potential

We investigated the effect of E141K and E141V on action potential (AP) morphology and dynamics exhibited by recombinant CaM-transfected iPSC-CMs. Representative spontaneous action potential traces show overt differences in action potential duration (APD) in cells expressing mutant CaM (**Fig. 6A**). Specifically, the APD_{90} and APD_{50} were significantly longer for E141K and E141V transfected iPSC-CM compared to WT expressing cells (**Fig. 6B,C**). Further, the proportional effect on APD_{50} was greater as reflected in a significantly smaller APD_{90}/APD_{50} ratio for iPSC-CM transfected with mutant CaM compared to WT CaM expressing cells **(Fig. 6D)**. This finding indicates prolongation of phase 2 repolarization where L-type Ca^{2+} current is prominent. The peak AP amplitude and the rate of rise (dV/dT) were significantly different in cells expressing E141K or E141V compared to WT expressing cells (**Supplemental Fig. S3A,B**). There was no difference between groups in maximum diastolic potential (**Supplemental Fig. S3C**) or in the frequency of spontaneous AP firing (**Supplemental Fig. S3D**). These results demonstrate that both E141K and E141V evoke prolonged action potential duration consistent with a cellular arrhythmogenic substrate underlying clinical LQTS.

DISCUSSION

In this study, we report two novel CaM mutations that affect the same amino acid residue in CaM but occur in two different genes. Both *CALM3*-E141K and *CALM1*-E141V cause impaired C-domain Ca^{2+} binding in recombinant CaM proteins, and cause a pattern of LTCC dysfunction consistent with impaired CDI. This study provides further evidence of the effect of CaM dysfunction on human cardiomyocyte electrophysiology, and supports dysregulation of LTCC as a pathogenic mechanism in calmodulinopathy presenting with LQTS. Importantly, we also report evidence of parental somatic mosaicism in the families with *CALM3*-E141K and *CALM3*-D130G, and these findings have important implications for genetic counseling in the setting of unexplained fetal demise or multiple sudden unexplained deaths of young children in families with a pathogenic CaM mutation.

Clinical aspects of calmodulinopathy-associated LQTS

CaM mutations associated with severe forms of LQTS potentiate the risk of sudden cardiac death in the young.[3,4,7,8,16] In a recent study, the average age at diagnosis of calmodulinopathy-associated LQTS was 0.8 years compared to 23 years in LQTS patients without CaM mutations.[4] In that same study, the average QTc interval duration was significantly longer in CaM mutation-positive patients (676 ms) compared to CaM mutation-negative patients (514ms), and the prevalence of sudden cardiac arrest (SCA) associated with calmodulinopathy was also significantly higher.

The two novel mutations we discovered affect the same residue of CaM (E141), and a third mutation at this position (*CALM1*-E141G) was previously reported.[4] All three substitutions of residue E141 are associated with severe LQTS. In Probands 1 and 2, who were both carriers of *CALM3*-E141K, the severity of LQTS based on QTc duration was more severe than Proband 3

(*CALM1*-E141V) and the published case with *CALM1*-E141G. Conceivably, the E141K mutation displays a more severe clinical phenotype than E141G or E141V because of side group charge differences in the mutant residue. Lysine substitution (E141K) introduces a positively charged residue that more severely disrupts Ca^{2+} binding affinity of the EF-hand motif compared to neutral glycine (E141G) and valine (E141V) substitutions (**Fig. 3**), which can be attributed to the more significant change in electrostatic interactions driving the binding of Ca^{2+} ions.

A potential novel clinical aspect of Proband 1 was the occurrence of hypoglycemia, which was the eventual cause of death. Although hypoglycemia has been reported in association with propranolol therapy in children, it is conceivable that altered L-type Ca^{2+} channel function in pancreatic β-cells as a consequence of the CaM mutation may have promoted hyperinsulinemia. A similar mechanism might explain hypoglycemia in Timothy syndrome,[19] which is caused by gain-of-function Ca^{2+} channel mutations.[20,21]

Proband 1 had documented left ventricle noncompaction (LVNC), an anatomic abnormality of the ventricle wall observed in a variety of genetic and acquired conditions as well as occasionally in healthy persons with normal heart size and function.[22] There have been four previous reports of calmodulinopathy accompanied by LVNC, all associated with *CALM2* mutations (D96V, D96G, D132E, D132H).[3,7,8,23] At the present time, there is insufficient evidence to suggest that LVNC is a direct or indirect consequence of CaM mutation. However, there have been prior associations with other genetic arrhythmia syndromes including CPVT associated with specific types of RYR2 mutations (exon 3 deletion).[24,25] Interestingly, in one case, LVNC developed subsequent to the worsening of cardiac arrhythmia.[25] It is conceivable that severe or progressive arrhythmic disorders associated with dysregulation of intracellular Ca^{2+} may predispose to this anomaly.

Cellular aspects of calmodulinopathy-associated LQTS

In our study, we used human iPSC-CM as a cellular model to determine the effect of E141K and E141V mutants on LTCC function and action potential morphology. Human iPSC-CM express endogenous LTCC and may have advantages over heterologous cellular platforms that require transfection of multiple subunit-encoding plasmids. This cellular model allows us to record Ca^{2+} currents and study action potential characteristics of cells expressing CaM mutations with a single plasmid transfection. Using this system, we demonstrated impaired Ca^{2+}-dependent regulation of LTCC inactivation, consistent with the cellular mechanism proposed for calmodulinopathy associated LQTS.[7,14,15] Human iPSC-CM also have utility as a cellular model to assess potential therapeutic strategies including gene therapies and targeted antiarrhythmic drugs.[15,26-28]

In addition to LTCC dysfunction, other cellular targets of CaM have been investigated to explain the pathogenesis of calmodulinopathies. Calmodulin mutations associated with CPVT are known to deregulate the RYR2 channel and cause arrhythmogenic spontaneous Ca^{2+} release.[9,29,30] Because our cases lacked overt features of CPVT, we did not pursue investigations of RYR2 function. Additional evidence supporting CaM-mediated dysregulation of the cardiac sodium channel ($Na_V1.5$) and the small-conductance Ca^{2+}–activated potassium channel (SK) channel has also been presented.[31] Enhanced $Na_V1.5$ late current was observed in heterologous cells transfected with the CaM mutant E141G,[4] but prior studies in cultured murine cardiomyocytes did not demonstrate effects on sodium current.[32]

Mosaicism in calmodulinopathy

An important and unique aspect of our study was the demonstration of parental mosaicism in two families. Mosaicism is an established genetic phenomenon that can explain recurrent mutation-positive offspring of apparently mutation-negative parents including in families with

LQTS.[33] The demonstration of mosaicism in our study was accomplished by 'deep' resequencing of the mutant gene using NGS technologies. In the family of Proband 1 (Fig. 2A), a mosaic mother carried the pathogenic variant (*CALM3*-p.E141K) in ~25% of NGS reads from peripheral blood cells. A similar degree of germline mosaicism would be consistent with the observed recurrent intrauterine fetal demise secondary to fetal calmodulinopathy in this family. However, this level of mosaicism in the heart would likely give rise to overt disease, and we speculate that cardiomyocytes exhibit a lower level of mosaicism to explain the absence of a maternal phenotype. By contrast, the family of Proband 4 (Fig. 2D) exhibits a high degree of recurrent cardiac arrhythmia among offspring that we presume is secondary to transmission of *CALM3*-p.D130G from the mosaic father, but in this case the proportion of mutation-positive NGS reads from peripheral blood was only ~6%. This degree of somatic mosaicism seems at odds with the high rate of disease recurrence among offspring in the family of Proband 4 suggesting that the proportion of mutation-positive peripheral blood cells may not reflect the level of mosaicism in the father's germline. We can also speculate that either the mutation was selectively amplified in the father's germline as was demonstrated previously for *FGFR2* mutations, or that sperm carrying the mutation had a selective advantage for fertilization.[34,35]

Conclusions

Calmodulin mutations are associated with a diversity of heart rhythm disorders, including LQTS, CPVT, idiopathic ventricular tachycardia, and sudden death. We report novel mutations associated with the LQTS and sudden death phenotypes, and demonstrated parental somatic mosaicism in two families. Our findings expand the mutational spectrum and add to the emerging genotype-phenotype correlation in this severe congenital arrhythmia syndrome.

ACKNOWLEDGEMENTS

The authors thank Defne E. Egecioglu and Tatiana Abramova for technical assistance.

FUNDING SOURCES

This work was supported by NIH grants HL083374 (A.L.G.), HL131914 (A.L.G.), GM118089 (W.J.C.), predoctoral (L.M.W.) and postdoctoral fellowships (C.N.J.) from the American Heart Association.

DISCLOSURES

A.L.G. serves on the Scientific Advisory Board of Amgen, Inc., and has received research funding from Merck, Xenon Pharmaceuticals, and Praxis Precision Medicines, Inc. for unrelated work. L.M. is a shareholder in Health in Code SL. All other authors declare no financial disclosures related to this work.

REFERENCES

1. George AL, Jr. Calmodulinopathy: a genetic trilogy. *Heart Rhythm.* 2015;12:423-424.

2. Nyegaard M, Overgaard MT, Sondergaard MT, Vranas M, Behr ER, Hildebrandt LL et al. Mutations in calmodulin cause ventricular tachycardia and sudden cardiac death. *Am J Hum Genet.* 2012;91:703-712.

3. Crotti L, Johnson CN, Graf E, De Ferrari GM, Cuneo BF, Ovadia M et al. Calmodulin mutations associated with recurrent cardiac arrest in infants. *Circulation.* 2013;127:1009-1017.

4. Boczek NJ, Gomez-Hurtado N, Ye D, Calvert ML, Tester DJ, Kryshtal D et al. Spectrum and Prevalence of CALM1-, CALM2-, and CALM3-Encoded Calmodulin (CaM) Variants in Long QT Syndrome (LQTS) and Functional Characterization of a Novel LQTS-Associated CaM Missense Variant, E141G. *Circ Cardiovasc Genet.* 2016;9:136-146.

5. Marsman RF, Barc J, Beekman L, Alders M, Dooijes D, van den WA et al. A mutation in CALM1 encoding calmodulin in familial idiopathic ventricular fibrillation in childhood and adolescence. *J Am Coll Cardiol.* 2014;63:259-266.

6. Kotta MC, Sala L, Ghidoni A, Badone B, Ronchi C, Parati G et al. Calmodulinopathy: A Novel, Life-Threatening Clinical Entity Affecting the Young. *Front Cardiovasc Med.* 2018;5:175.

7. Pipilas DC, Johnson CN, Webster G, Schlaepfer J, Fellmann F, Sekarski N et al. Novel calmodulin mutations associated with congenital long QT syndrome affect calcium current in human cardiomyocytes. *Heart Rhythm.* 2016;13:2012-2019.

8. Makita N, Yagihara N, Crotti L, Johnson CN, Beckmann BM, Roh MS et al. Novel calmodulin mutations associated with congenital arrhythmia susceptibility. *Circ Cardiovasc Genet.* 2014;7:466-474.

9. Gomez-Hurtado N, Boczek NJ, Kryshtal DO, Johnson CN, Sun J, Nitu FR et al. Novel CPVT-associated calmodulin mutation in CALM3 (CALM3-A103V) activates arrhythmogenic Ca waves and sparks. *Circ Arrhythm Electrophysiol.* 2016;9.

10. Zahavich L, Tarnopolsky M, Yao R, Mital S. Novel association of a de novo CALM2 mutation with long QT syndrome and hypertrophic cardiomyopathy. *Circ Genom Precis Med.* 2018;11:e002255.

11. Berchtold MW, Egli R, Rhyner JA, Hameister H, Strehler EE. Localization of the human bona fide calmodulin genes CALM1, CALM2, and CALM3 to chromosomes 14q24-q31, 2p21.1-p21.3, and 19q13.2-q13.3. *Genomics.* 1993;16:461-465.

12. Fischer R, Koller M, Flura M, Mathews S, Strehler-Page MA, Krebs J et al. Multiple divergent mRNAs code for a single human calmodulin. *J Biol Chem.* 1988;263:17055-17062.

13. Watterson DM, Sharief F, Vanaman TC. The complete amino acid sequence of the Ca^{2+}-dependent modulator protein (calmodulin) of bovine brain. *J Biol Chem.* 1980;255:962-975.

14. Limpitikul WB, Dick IE, Joshi-Mukherjee R, Overgaard MT, George AL, Jr., Yue DT. Calmodulin mutations associated with long QT syndrome prevent inactivation of cardiac L-type Ca currents and promote proarrhythmic behavior in ventricular myocytes. *J Mol Cell Cardiol.* 2014;74:115-124.

15. Rocchetti M, Sala L, Dreizehnter L, Crotti L, Sinnecker D, Mura M et al. Elucidating arrhythmogenic mechanisms of long-QT syndrome CALM1-F142L mutation in patient-specific induced pluripotent stem cell-derived cardiomyocytes. *Cardiovasc Res.* 2017;113:531-541.

16. Reed GJ, Boczek NJ, Etheridge SP, Ackerman MJ. CALM3 mutation associated with long QT syndrome. *Heart Rhythm.* 2015;12:419-422.

17. Hiatt JB, Pritchard CC, Salipante SJ, O'Roak BJ, Shendure J. Single molecule molecular inversion probes for targeted, high-accuracy detection of low-frequency variation. *Genome Res.* 2013;23:843-854.

18. Carlstrom G, Chazin WJ. Two-dimensional 1H nuclear magnetic resonance studies of the half-saturated (Ca^{2+})1 state of calbindin D9k. Further implications for the molecular basis of cooperative Ca^{2+} binding. *J Mol Biol.* 1993;231:415-430.

19. George AL, Jr. The importance of being selective. *Heart Rhythm.* 2019;16:279-280.

20. Splawski I, Timothy KW, Sharpe LM, Decher N, Kumar P, Bloise R et al. $Ca_V1.2$ calcium channel dysfunction causes a multisystem disorder including arrhythmia and autism. *Cell.* 2004;119:19-31.

21. Splawski I, Timothy KW, Decher N, Kumar P, Sachse FB, Beggs AH et al. Severe arrhythmia disorder caused by cardiac L-type calcium channel mutations. *Proc Natl Acad Sci U S A.* 2005;102:8089-8096.

22. Arbustini E, Favalli V, Narula N, Serio A, Grasso M. Left Ventricular Noncompaction: A Distinct Genetic Cardiomyopathy? *J Am Coll Cardiol.* 2016;68:949-966.

23. Crotti L, Spazzolini C, Tester DJ, Ghidoni A, Baruteau AE, Beckmann BM et al. Calmodulin mutations and life-threatening cardiac arrhythmias: insights from the International Calmodulinopathy Registry. *Eur Heart J.*, doi:10.1093/eurheartj/ehz311.

24. Ohno S, Omura M, Kawamura M, Kimura H, Itoh H, Makiyama T et al. Exon 3 deletion of RYR2 encoding cardiac ryanodine receptor is associated with left ventricular non-compaction. *Europace.* 2014;16:1646-1654.

25. Campbell MJ, Czosek RJ, Hinton RB, Miller EM. Exon 3 deletion of ryanodine receptor causes left ventricular noncompaction, worsening catecholaminergic polymorphic ventricular tachycardia, and sudden cardiac arrest. *Am J Med Genet A.* 2015;167A:2197-2200.

26. Limpitikul WB, Dick IE, Tester DJ, Boczek NJ, Limphong P, Yang W et al. A precision medicine approach to the rescue of function on malignant calmodulinopathic long-QT syndrome. *Circ Res.* 2017;120:39-48.

27. Yamamoto Y, Makiyama T, Harita T, Sasaki K, Wuriyanghai Y, Hayano M et al. Allele-specific ablation rescues electrophysiological abnormalities in a human iPS cell model of long-QT syndrome with a CALM2 mutation. *Hum Mol Genet.* 2017;26:1670-1677.

28. Schwartz PJ, Gnecchi M, Dagradi F, Castelletti S, Parati G, Spazzolini C et al. From patient-specific induced pluripotent stem cells to clinical translation in long QT syndrome Type 2. *Eur Heart J.* 2019;40:1832-1836.

29. Hwang HS, Nitu FR, Yang Y, Walweel K, Pereira L, Johnson CN et al. Divergent regulation of RyR2 calcium release channels by arrhythmogenic human calmodulin missense mutants. *Circ Res.* 2014;114:1114-1124.

30. Sondergaard MT, Tian X, Liu Y, Wang R, Chazin WJ, Chen SR et al. Arrhythmogenic calmodulin mutations affect the activation and termination of cardiac ryanodine receptor-mediated Ca^{2+} release. *J Biol Chem.* 2015;290:26151-26162.

31. Yu CC, Ko JS, Ai T, Tsai WC, Chen Z, Rubart M et al. Arrhythmogenic calmodulin mutations impede activation of small-conductance calcium-activated potassium current. *Heart Rhythm.* 2016;13:1716-1723.

32. Yin G, Hassan F, Haroun AR, Murphy LL, Crotti L, Schwartz PJ et al. Arrhythmogenic calmodulin mutations disrupt intracellular cardiomyocyte Ca^{2+} regulation by distinct mechanisms. *J Am Heart Assoc.* 2014;3:e000996.

33. Schwartz PJ. Stillbirths, sudden infant deaths, and long-QT syndrome: puzzle or mosaic, the pieces of the jigsaw are being fitted together. *Circulation.* 2004;109:2930-2932.

34. Choi SK, Yoon SR, Calabrese P, Arnheim N. A germ-line-selective advantage rather than an increased mutation rate can explain some unexpectedly common human disease mutations. *Proc Natl Acad Sci U S A.* 2008;105:10143-10148.

35. Goriely A, McVean GA, Rojmyr M, Ingemarsson B, Wilkie AO. Evidence for selective advantage of pathogenic FGFR2 mutations in the male germ line. *Science.* 2003;301:643-646.

FIGURE LEGENDS

Figure 1. Abnormal electrocardiographic traces from probands.

A. Twelve-lead ECG traces obtained at birth for Proband 1 illustrating sinus bradycardia, a prolonged QTc interval (725 ms), and 2:1 AV block. **B.** An episode of T-wave alternans recorded from Proband 1 is illustrated. **C.** ECG rhythm during resuscitation of Proband 1 from VF cardiac arrest on the 23rd day of life. **D.** ECG trace recorded at age 2 weeks from Proband 2 showing a QTc of 660 ms. **E.** ECG trace recorded at age 18 months from Proband 3 showing a QTc of 630 ms and inverted T waves throughout the precordial leads. **F.** ECG trace from Proband 4 recorded at age 4 days showing a QTc of 505 ms and 2:1 AV block.

Figure 2. Pedigrees of calmodulinopathy families and discovery of novel CaM mutations.

A-D. Pedigrees representing the family structures of Probands 1-4. Males are represented as square symbols, females as circles, miscarriages as triangles, elective abortions as triangles with diagonal lines. The QTc or phenotype, and *CALM3* genotype are given below each pedigree symbol. In Family D, age of sudden death (SD) is given. Individuals unavailable for genotyping are labeled as 'No DNA'. **E.** Nucleotide sequencing traces showing heterozygous mutations in *CALM3* for Proband 1 (Family A, II.1) and the mosaic mother (I.2), and heterozygous mutation in *CALM1* for Proband 2 (Family C, II.1) compared to a normal genotype in the father (I.1).

Figure 3. E141K and E141V reduce Ca^{2+} binding affinity of the calmodulin C-lobe.

A. Amino acid sequence alignments comparing a segment of the CaM C-domain from different species (*left*) and a schematic of the 4th EF-hand motif showing the location of the E141K and E141V mutations (*right*). **B.** An overlay of WT (*black*), E141K (*red*), and E141V (*blue*) fluorescence change during Ca^{2+} titration for the CaM C-domain. **C.** Normalized fluorescence

change for Ca^{2+} titration experiments. The Ca^{2+} affinities (Kd) for the CaM C-domain are provided in the inset.

Figure 4. Effect of E141K and E141V CaM on iPSC-CM Ca^{2+} current.

A. Average traces of Ca^{2+} current recorded from iPSC-CMs transfected with CaM-WT (*top*), CaM-E141K (*middle*), or CaM-E141V (*bottom*). **B.** Current density *vs* voltage plot comparing the peak Ca^{2+} current of WT, E141K, and E141V expressing cells (#, $p < 0.05$, E141K *vs* WT). **C.** Current density *vs* voltage plot comparing the late Ca^{2+} current recorded 100 ms after each voltage step (*, $p < 0.05$, both mutants *vs* WT; #, $p < 0.05$, E141K *vs* WT). Data symbols represent mean values of WT (n=17), E141K (n=10), and E141V (n=8) expressing cells and error bars are standard error of the mean (SEM).

Figure 5. E141K and E141V impair Ca^{2+}-dependent inactivation.

A. Average traces of Ca^{2+} (*black*) and Ba^{2+} (*red*) current recorded at +10 mV from iPSC-CMs transfected with CaM-WT (*top*), CaM-E141K (*middle*), or CaM-E141V (*bottom*). **B.** Plots of I_{end}/I_{peak} for test voltages between -10 to +50 mV (*, $p < 0.05$, both mutants *vs* WT; #, $p < 0.05$, E141K *vs* WT). Data symbols represent mean values of WT (n=17), E141K (n=10), and E141V (n=8) and error bars are standard error of the mean (SEM).

Figure 6. E141K and E141V prolong the action potential duration in iPSC-CM.

A. Representative traces of action potentials recorded from human iPSC-CMs transfected with CALM3 WT or E141K (*top*), or with CALM1 WT or E141V (*bottom*). **B.** Box plots of action potential duration at 90% repolarization (APD_{90}) of spontaneous APs in cells expressing E141K or E141V compared to WT expressing cells. The vertical height of each box plot represents the 25^{th} to 75^{th} percentile, the solid black line within the box marks the median, and the mean value is indicated by the dashed line with the box. Whiskers (error bars) above and below the box indicate the 95^{th} and 5^{th} percentiles, respectively. All data points are plotted. **C.** Box plots of

action potential duration at 50% repolarization (APD_{50}) of spontaneous APs in cells expressing E141K or E141V compared to WT expressing cells. **D.** Box plots depicting ratios of APD_{90} to APD_{50} determined for spontaneous AP (*, $p < 0.05$, comparing mutant to WT).

Table 1: Clinical and genetic features of probands with calmodulinopathy.

Proband	Mutation	Inheritance	QTc (ms)	Sex	Age Onset (days)	Phenotype
1	*CALM3*-E141K	mosaic	725	F	1	Fetal bradycardia, SCA, LQTS, 2:1 AV block
2	*CALM3*-E141K	*de novo*	660	M	1	Bradycardia, syncope, LQTS, 2:1 AV block
3	*CALM1*-E141V	*de novo*	630	M	28	Syncope, LQTS, VT/VF
4	*CALM3*-D130G	mosaic	505	M	4	VT/VF, LQTS, 2:1 AV block, SCD

Abbreviations: LQTS = long QT syndrome; SCA = sudden cardiac arrest; SCD = sudden cardiac death; VT/VF – ventricular tachycardia/fibrillation

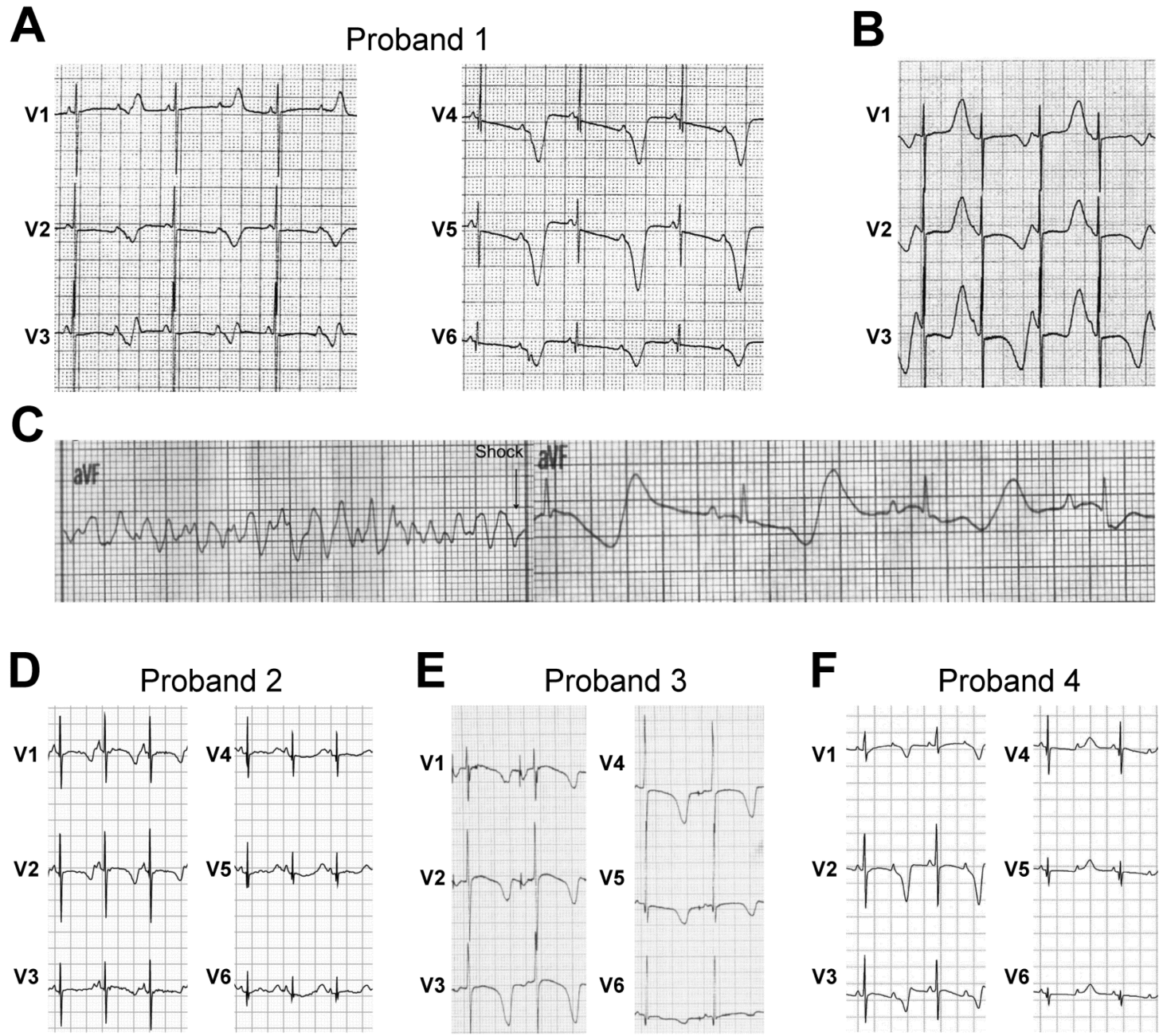
A
Proband 1
V1
V2
V3
V4
V5
V6
B
V1
V2
V3
C
aVF
Shock
aVF
D
Proband 2
V1
V2
V3
V4
V5
V6
E
Proband 3
V1
V2
V3
V4
V5
V6
F
Proband 4
V1
V2
V3
V4
V5
V6

Figure 1

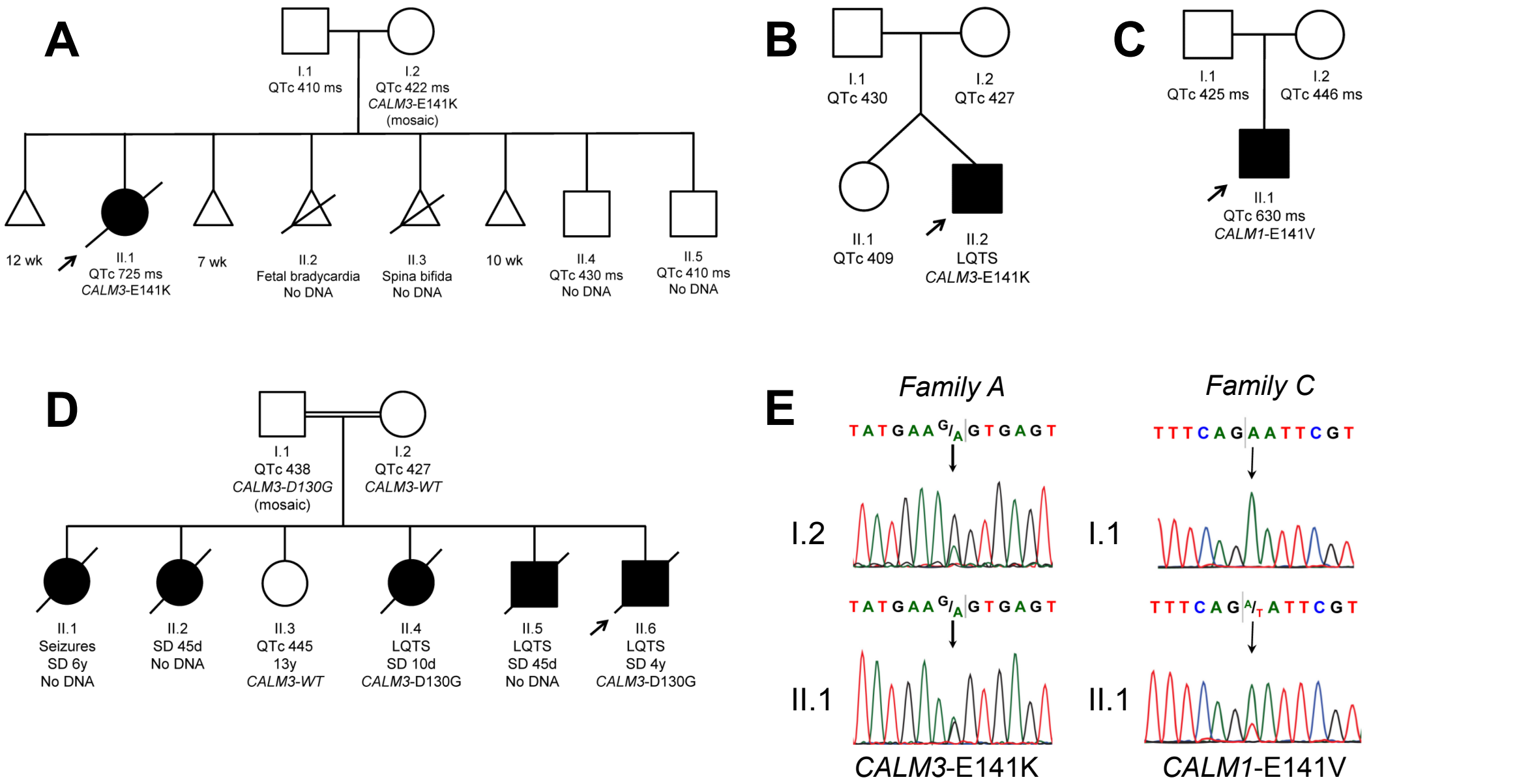
A
I.1
QTc 410 ms
I.2
QTc 422 ms
CALM3-E141K
(mosaic)
12 wk
II.1
QTc 725 ms
CALM3-E141K
7 wk
II.2
Fetal bradycardia
No DNA
II.3
Spina bifida
No DNA
10 wk
II.4
QTc 430 ms
No DNA
II.5
QTc 410 ms
No DNA
B
I.1
QTc 430
I.2
QTc 427
II.1
QTc 409
II.2
LQTS
CALM3-E141K
C
I.1
QTc 425 ms
I.2
QTc 446 ms
II.1
QTc 630 ms
CALM1-E141V
D
I.1
QTc 438
CALM3-D130G
(mosaic)
I.2
QTc 427
CALM3-WT
II.1
Seizures
SD 6y
No DNA
II.2
SD 45d
No DNA
II.3
QTc 445
13y
CALM3-WT
II.4
LQTS
SD 10d
CALM3-D130G
II.5
LQTS
SD 45d
No DNA
II.6
LQTS
SD 4y
CALM3-D130G
E
Family A
Family C
I.2
I.1
II.1
II.1
CALM3-E141K
CALM1-E141V

Figure 2

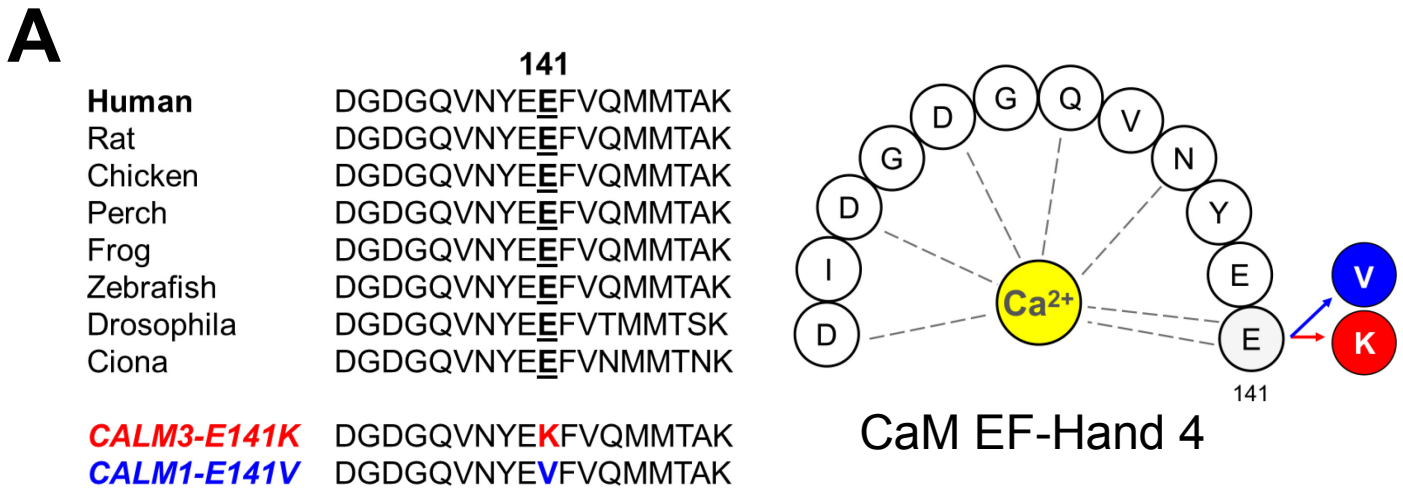
A
141
Human DGDGQVNYEEFVQMMTAK
Rat DGDGQVNYEEFVQMMTAK
Chicken DGDGQVNYEEFVQMMTAK
Perch DGDGQVNYEEFVQMMTAK
Frog DGDGQVNYEEFVQMMTAK
Zebrafish DGDGQVNYEEFVQMMTAK
Drosophila DGDGQVNYEEFVTMMTSK
Ciona DGDGQVNYEEFVNMMTNK
CALM3-E141K DGDGQVNYEKFVQMMTAK
CALM1-E141V DGDGQVNYEVFVQMMTAK
D G Q V N Y E E K V
D G D I D
Ca2+
141
CaM EF-Hand 4

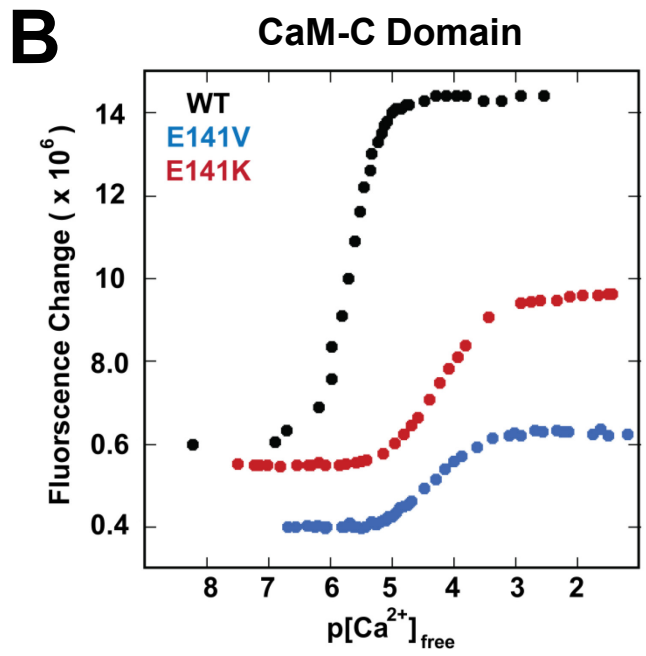
B
CaM-C Domain
WT
E141V
E141K
Fluorscence Change (x 10^6)
14
12
10
8.0
0.6
0.4
8 7 6 5 4 3 2
p[Ca2+]free

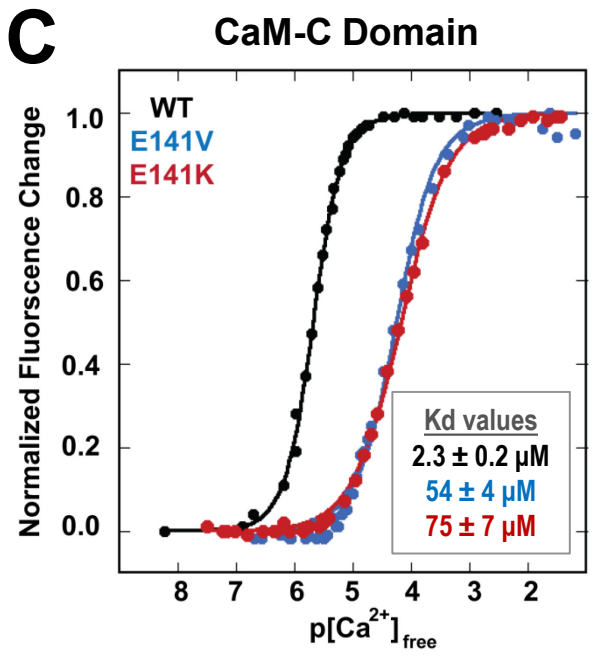
C
CaM-C Domain
WT
E141V
E141K
Normalized Fluorscence Change
1.0
0.8
0.6
0.4
0.2
0.0
Kd values
2.3 ± 0.2 µM
54 ± 4 µM
75 ± 7 µM
8 7 6 5 4 3 2
p[Ca2+]free

Figure 3

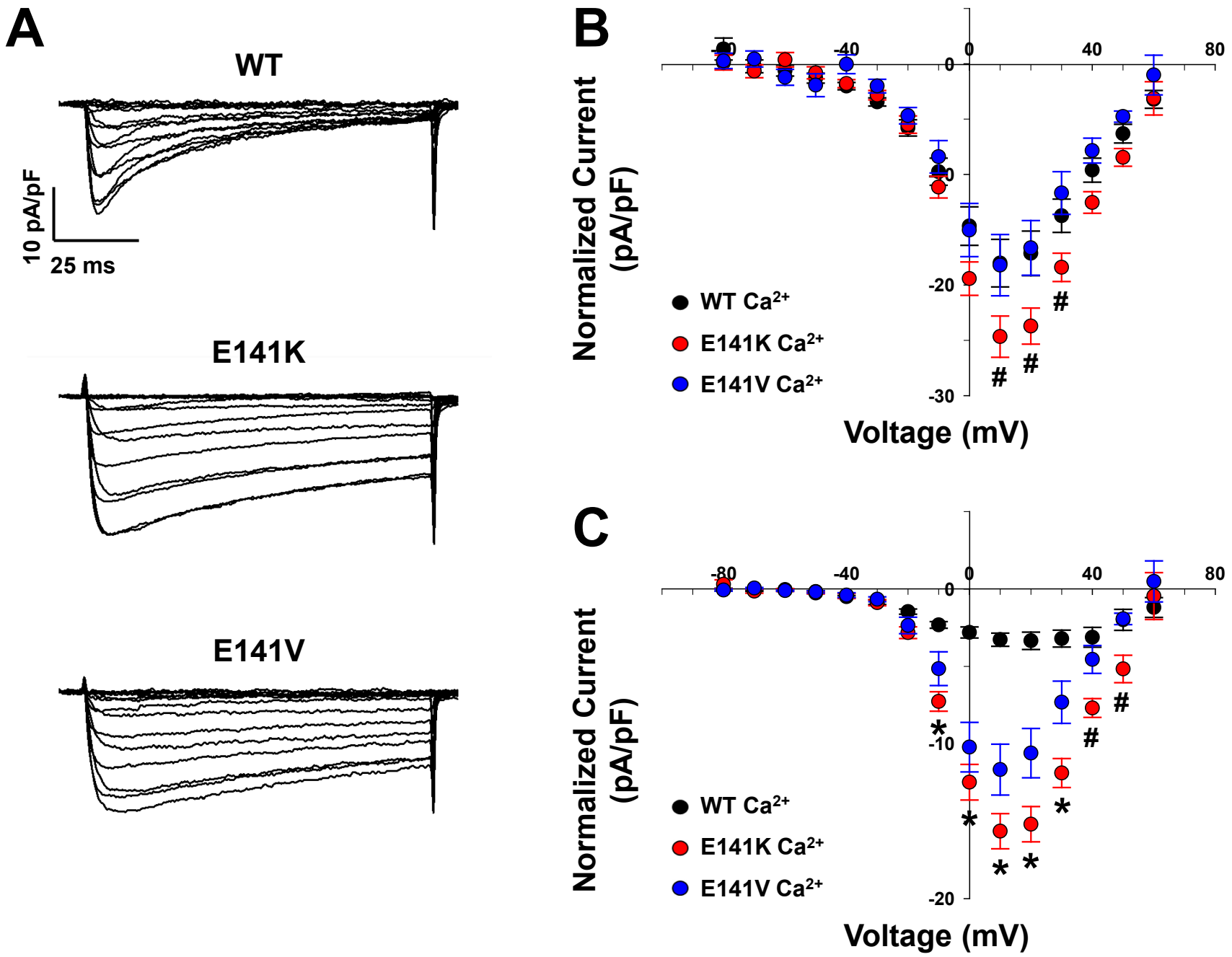
A
WT
10 pA/pF
25 ms
E141K
E141V
B
Normalized Current (pA/pF)
WT Ca2+
E141K Ca2+
E141V Ca2+
Voltage (mV)
C
Normalized Current (pA/pF)
WT Ca2+
E141K Ca2+
E141V Ca2+
Voltage (mV)

Figure 4

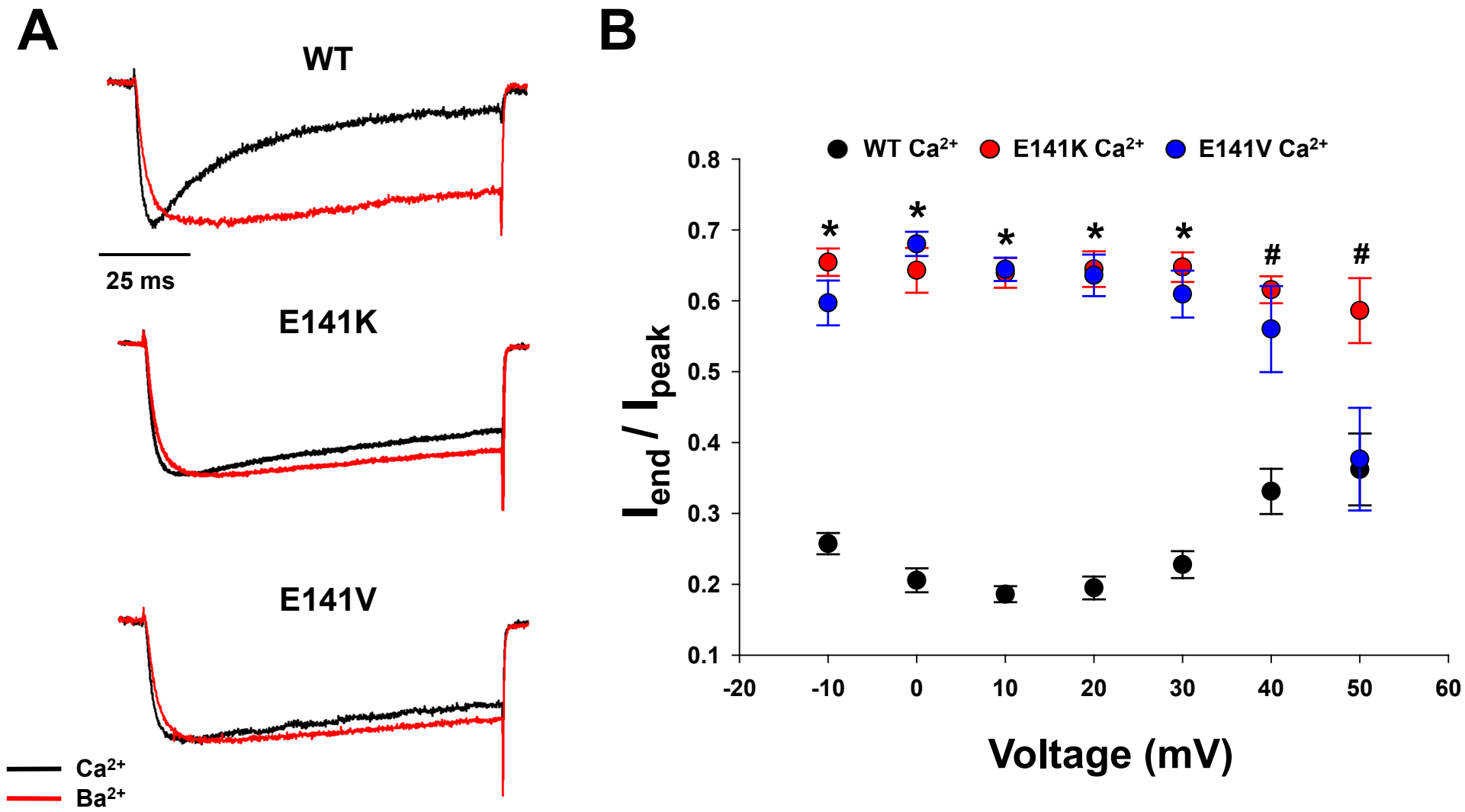
A
WT
25 ms
E141K
E141V
Ca2+
Ba2+
B
WT Ca2+
E141K Ca2+
E141V Ca2+
Iend / Ipeak
Voltage (mV)
0.8
0.7
0.6
0.5
0.4
0.3
0.2
0.1
-20
-10
0
10
20
30
40
50
60
*
#

Figure 5

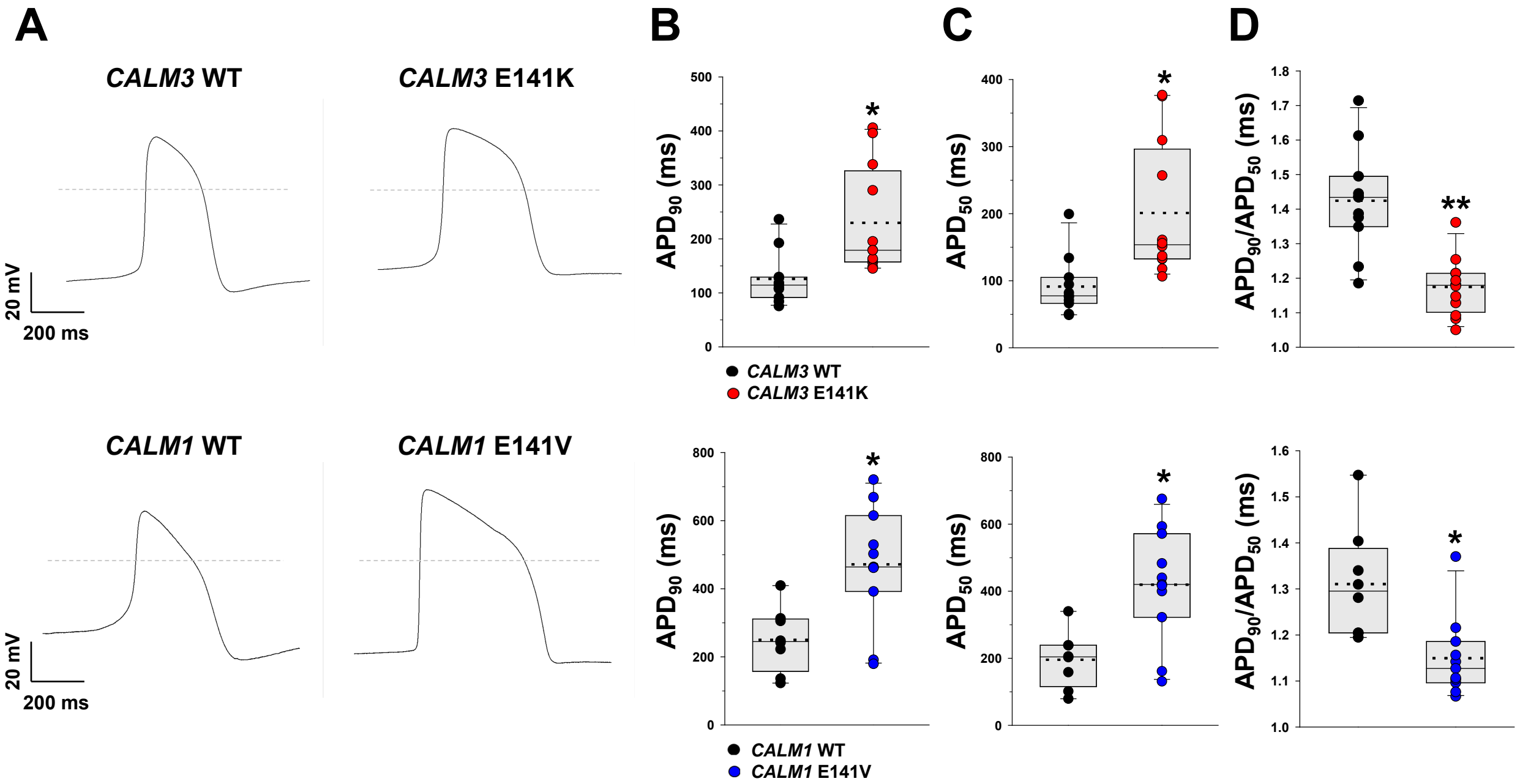
A
CALM3 WT
CALM3 E141K
20 mV
200 ms
CALM1 WT
CALM1 E141V
20 mV
200 ms
B
APD90 (ms)
CALM3 WT
CALM3 E141K
CALM1 WT
CALM1 E141V
C
APD50 (ms)
D
APD90/APD50 (ms)

Figure 6